Different pathways in mechanical unfolding/folding cycle of a single semiflexible polymer

Natsuhiko Yoshinaga and Kenichi Yoshikawa

Department of Physics, Graduate School of Sciences,

Kyoto University, Kyoto 606-8502, Japan

Takao Ohta

Yukawa Institute for Theoretical Physics,

Kyoto University, Kyoto 606-8502, Japan

(Dated: February 2, 2008)

Abstract

Kinetics of conformational change of a semiflexible polymer under mechanical external field were investigated with Langevin dynamics simulations. It is found that a semiflexible polymer exhibits large hysteresis in mechanical folding/unfolding cycle even with a slow operation, whereas in a flexible polymer, the hysteresis almost disappears at a sufficiently slow operation. This suggests that the essential features of the structural transition of a semiflexible polymer should be interpreted at least on a two-dimensional phase space. The appearance of such large hysteresis is discussed in relation to different pathways in the loading and unloading processes. By using a minimal two-variable model, the hysteresis loop is described in terms of different pathways on the transition between two stable states.

PACS numbers: 36.20.-r,87.15.La,05.70.Fh

I. INTRODUCTION

Recent developments in experimental techniques regarding single molecule observation and manipulation have enabled us to directly investigate the statistical properties of individual small systems.[1, 2] These experiments have provided novel insights into the structure and function of biological macromolecules. These studies have revealed significant effects of fluctuation on the properties of single molecules.

Most biopolymers, including DNA and many proteins, have finite stiffness and are therefore classified as semiflexible polymers. It is expected that the stiffness plays an important role in the structural stability and function of these biomacromolecules. Recent experiments and simulations have clarified that a single semiflexible polymer exhibits first order phase transition between elongated coil and folded compact states with a decrease in the solvent quality.[3] A single semiflexible polymer folds into various kinds of ordered structures depending on its stiffness and temperature, such as a toroid or a rod.[4] This implies that the density of monomers is not sufficient to characterize ordered structures, but the orientational order plays an essential role in the folding transition of a semiflexible chain, i.e., the density-order coupling should be crucial.

Among the studies on single molecule manipulation, experiments on mechanical unfolding with laser tweezers or atomic force microscopy have been actively performed over the past decade. [5, 6, 7] In these experiments, a non-trivial force response, which is called a *sawtooth-like* pattern or a *stick-and-release* pattern, has been observed either in a protein or in a DNA molecule. Some authors claim that such patterns are associated with repeated domain structures in a molecule.[8, 9] In contrast to this, it is found in [6, 7] that a DNA molecule having no repeated sequence exhibits a *stick-and-release* pattern at the collapsing conditions where the concentration of multivalent cations is high, whereas the mechanical response of a worm-like chain is observed when a DNA molecule is in the coil conditions at the low concentration of multivalent cations. Furthermore, it has been argued theoretically that a toroidal structure of a folded semiflexible polymer without any repeated domains leads to a *stick-and-release* pattern.[10, 11]

A system under loading and unloading processes is clearly in a nonequilibrium state unless the rate of change is infinitesimally slow, and therefore the kinetics play essential roles. Recently, it has been revealed that a difference in the equilibrium free energy can

be calculated from kinetic processes under a nonequilibrium state[12, 13] and the theory has been applied to biopolymer stretching.[14] Despite such an analysis of nonequilibrium effects, there have been few studies on the large hysteresis loop observed in the loading and unloading cycle of biomolecules.

Hysteresis is a measure of how the system is away from thermal equilibrium. At the length scale of micron or submicron, thermalization is so fast that equilibrium states are easily attained. However, to perform work against an external force, as seen with molecular motors in biological systems, the system should remain in a nonequilibrium state. Therefore, it is important to clarify the origin of hysteresis and, especially, its robustness.

Theoretical and numerical studies are needed to gain general insight into not only the nonequilibrium characteristics of a single polymer chain, but also the working mechanism of a macromolecule in biological systems. In the present article, we consider flexible and semi-flexible polymers under strain by molecular dynamics simulations. We investigate the force response and focus on the close connection between hysteresis and the structural transition of a single polymer chain.

A coarse-grained approach is generally quite useful to understand the essence of the phase transitions. We shall introduce a Ginzburg-Landau type free energy and the kinetic equations for the present problem. As mentioned above, however, the density of monomers is not sufficient to distinguish the different conformation in a semiflexible chain. Therefore, we introduce another kinetic variable corresponding to the orientational order. We do not intend to derive the free energy starting from the chain model but show that the coarse-grained free energy having two metastable states indeed describes properly the hysteresis in the force-response relation. To our knowledge, this kind of approach has not been available in the kinetics of a single chain.

In the next section, we present our chain model and describe the method of simulations. In section III, the results of simulations are given. A phenomenological scaling argument is developed in section IV. The two-variable model and its numerical studies are shown in section V. A summary is given in section VI.

II. SIMULATIONS

To examine the folding and unfolding kinetics, we carried out Langevin dynamics simulations of a bead-spring model using the following potentials

$$V_{\text{beads}} = \frac{k_a}{2} \sum_i (|\mathbf{r}_{i+1} - \mathbf{r}_i| - a)^2 \tag{1}$$

$$V_{\text{bend}} = \frac{\kappa}{2} \sum_i (1 - \cos\theta_i)^2 \tag{2}$$

$$V_{\text{LJ}} = 4\epsilon \sum_{i,j} ((\frac{a}{|\mathbf{r}_i - \mathbf{r}_j|})^{12} - (\frac{a}{|\mathbf{r}_i - \mathbf{r}_j|})^6), \tag{3}$$

where $V = V_{\text{beads}} + V_{\text{bend}} + V_{\text{LJ}}$ and $\mathbf{r}_i$ is the coordinate of the ith monomer and θ_i is the angle between adjacent bond vectors. The monomer size a and $k_B T$ are chosen as the unit length and energy, respectively, where k_B is the Boltzmann constant and T is the absolute temperature. Monomer-monomer interaction is included by the Lennard-Jones potential controlled by ϵ. A similar bead-spring model (1) - (3) has been used to study the properties of semiflexible chains by setting a large value of k_a.[15] We adopt the parameters to be $k_a = 400$ and $\epsilon = 1.0$. The bending elasticity is chosen to be $\kappa = 100$ for a semiflexible polymer and $\kappa = 0$ for a flexible polymer. The persistence length l_p is a convenient measure to characterize the stiffness of a polymer chain. In the present model, $l_p \sim 13.5a$ for a semiflexible polymer. Because of discritization of a chain with beads, the minimum of the persistence length is a, and therefore $l_p \sim a$ for a flexible polymer. We consider a homopolymer with a polymerization index $N = 200$.

A remark is now in order. Because a semiflexible chain is locally inextensible, the partition function should be written as $Z = \int \mathcal{D}\mathbf{r}_i \Pi \delta(|\mathbf{r}_{i+1} - \mathbf{r}_i| - a)e^{-(V_{\text{bend}}+V_{\text{LJ}})}$. As an analytically or numerically tractable model, several approximations have been employed and examined. For example, the local constraint was replaced by a global constraint in refs.[16, 17] to study analytically the equilibrium properties of a semiflexible polymer. Instead of such approximations, we adapt the harmonic potential (1) between a pair of the neighboring beads. A continuum version of the model (1) was introduced to evaluate the end-to-end distance[18] which shows clearly that the end-to-end distance is insensitive to k_a for large values of k_a.

The equation of motion can be written as,

$$m\frac{d^2\mathbf{r}_i}{dt^2} = -\gamma\frac{d\mathbf{r}_i}{dt} - \frac{\partial V}{\partial \mathbf{r}_i} + \boldsymbol{\xi}_i, \tag{4}$$

where m and γ are the mass and friction constant of a monomeric unit, respectively. The constant $\tau = \gamma a^2/k_B T$ is chosen to be the unit for the time scale. We set the time step as 0.01τ, and use $m = 1.0$ and $\gamma = 1.0$. Gaussian white noise $\boldsymbol{\xi_i}$ satisfies a fluctuation-dissipation relation,

$$< \boldsymbol{\xi}_i(t) \cdot \boldsymbol{\xi}_j(t') > = 6\gamma k_B T \delta_{ij} \delta(t - t'), \tag{5}$$

where $< \cdots >$ indicates an ensemble average.

The folding and unfolding states of a polymer are characterized by the average local monomer density ρ, which is defined by,

$$\rho = \frac{1}{N} \sum_{i,j} H(r_c^2 - |\mathbf{r}_i - \mathbf{r}_j|^2), \tag{6}$$

where $H(x)$ is the Heaviside function. In this work, we set $r_c = 3.0$.

Several comments on the values of the parameters chosen above are in order. The attractive strength ϵ in the Lennard-Jones potential (3) is chosen so that ordered structures such as toroids and rods are formed for polymerization index $N = 200$ and $l_p \sim 13.5a$.[4] Among such ordered structures, a toroidal structure is the most energetically favorable in the present set of parameters. The spring constant k_a in (1) is set to be a sufficiently large value to realize the local inextensibility of a chain. We set $m = \gamma = 1.0$ in (4) to optimize the numerical simulations within accessible simulation time avoiding any numerical instabilities. With this condition, the inertia term does not cause any artifacts because the relaxation time of the momentum of a monomer is sufficiently faster compared to that of conformational change.

We fix one end of a polymer chain and move the other end at constant velocity $\dot{z}$. The end-to-end distance z is one of the measurable quantities. The force f applied to the Nth monomer is monitored during the operation. Note that force is averaged over time to avoid its large fluctuation. The inverse velocity $\lambda = \dot{z}^{-1}$ is often used as a measure of the speed of external operations. It is convenient to define λ_{fold}, which corresponds to the time scale of the folding transition of a semiflexible polymer in bulk. It can be written as $\lambda_{\text{fold}} = < \tau_{\text{fold}}/(R_{\text{coil}} - R_{\text{fold}}) >$, where τ_{fold} is the characteristic time for a folding transition, and R_{coil} and R_{fold} are the end-to-end distance of the coiled and folded states in a semiflexible polymer, respectively.

Here we mention the time and length scales in our simulations. The advantage of the bead-spring model (4) with (1-3) is that we can simulate on a realistic time scale. The folding

transition time is on the order of $10^5 - 10^6$ steps, which corresponds to about 0.1 - 1.0 sec in the experiment with DNA.[19] From this correspondence, our loading and unloading speed ($10^7 - 10^8$ steps in the simulations) is considered to correspond to 10 - 100 sec, which is a experimentally accessible value. We can also discuss the length scale. The persistence length of DNA is about 50 nm, which corresponds to about $10a$ in our simulation. Therefore, we can estimate the size of a toroidal state of a semiflexible polymer ($\sim 10a$ in the simulation) to be about 50 nm, which is in good agreement with experiments on DNA. Most simulations suffer from a large value of the force response.[20] However, the force response in our simulations ($2a - 5a/k_BT$) corresponds to $3 - 7$pN, which is consistent with the experimental value. [7]

III. RESULTS

Figure 1 shows the local monomer density and the force response of a flexible polymer and a semiflexible polymer, where the former takes a spherical globule morphology and the latter takes a toroidal morphology in their compact states. We have chosen the inverse velocity as $\lambda = 10^4\tau/a$ in Fig.1. It can be seen that the pathway of structural transition in the loading of a semiflexible polymer is clearly different from that in unloading.

The force response in a flexible polymer increases at $z < 20$, maintains a constant value at $20 < z < 80$, and then increases at $z > 80$. Correspondingly, a globular flexible polymer changes to an ellipsoidal shape and then to a phase-segregated state consisting of a coil and a globule, followed by a coil state. This behavior is observed in both loading and unloading, and thus a flexible polymer does not exhibit hysteresis. The force response observed in Fig.1B(b) is called a *force plateau*, and was predicted by Halperin et al.[21, 22]

In the loading of a semiflexible polymer, a toroidal semiflexible polymer shows phase segregation of a coil and a toroid part. In this state, the monomer density decreases in a stepwise manner, and correspondingly the force response exhibits a *stick-and-release pattern*, which has been observed in experiments with DNA.[6, 7] At $z \sim 140$, the polymer undergoes a transition to a coiled state. In the unloading process, on the other hand, the phase-separated state of a rod and a coil appears at $z \sim 125$, and the polymer becomes a single phase consisting of a rod. At the final stage, a rod becomes more folded or makes a transition to a toroid. The force response in a rod-coil phase-segregated state exhibits a *force plateau* and is largely different from that in a toroid-coil state.

6

Next, we consider the cycle in which the initial and final states are coiled states. As shown in Fig.2, a semiflexible polymer exhibits a large hysteresis loop, in contrast to a flexible polymer. To see the difference more quantitatively, we calculate the hysteresis area at various operating speeds. Figure 3 shows the hysteresis area of the force response, i.e. the difference in dissipative work between loading and unloading processes. In a flexible polymer, hysteresis rapidly decreases as the operating speed decreases. In contrast, hysteresis in a semiflexible polymer decreases rather slowly. Large hysteresis remains even at $\lambda \sim 10^4 \tau/a$, although a semiflexible polymer in bulk makes a transition to a folded state on the time scale $\lambda_{\mathrm{fold}} \sim 2 \times 10^2 \tau/a$. Therefore, we conclude that a semiflexible polymer maintains large hysteresis even at an extremely slow operation speed.

The appearance of notable hysteresis in a semiflexible polymer is associated with the significant difference in the pathways between the loading and unloading processes. In unloading, a rod-like structure appears frequently, whereas in loading, a toroidal loop structure tends to be generated. As shown in Figs.1 and 2, the force response strongly depends on the structure of the folded part. This structural difference is the origin of the large hysteresis in a semiflexible polymer. In contrast, there is almost no difference in the transition pathways of a flexible polymer between the loading and unloading processes (Fig.2C).

Obviously, the hysteresis should disappear at the infinitesimally slow operation where the transition between a toroid and a rod is achieved. However in a practical sense, it is difficult to observe the transition because of a large free energy barrier between these states.

IV. SCALING ANALYSIS

In this section, we will discuss physical meanings of the hysteresis appearing in the cycle. Energy balance can be written with the work $\mathrm{d}W$ per unit time by the external perturbation as,

$$\mathrm{d}W = \mathrm{d}F + \mathrm{d}Q, \tag{7}$$

where the first and second terms in the r.h.s. are free energy change and dissipative heat, respectively. The hysteresis area A in the present system corresponds to the difference between total works in loading and unloading process, $A = |W_{\mathrm{load}}| - |W_{\mathrm{unload}}|$. The dissipative heat is equivalent to the entropy production of solvent molecules,

$$\mathrm{d}Q = \mathrm{d}S. \tag{8}$$

7

In the estimation of the entropy production, only the Stokes drag is considered because the hydrodynamic interaction is neglected in the present work.

We consider a polymer which consists of coiled and collapsed parts. The coiled part has n unfolded monomers, and is l in size in the direction parallel to the external force and R in the perpendicular direction. The collapsed part is either globule, toroid or rod state. The main contribution to the entropy production comes from the coiled part and is

$$\frac{\mathrm{d}S}{\mathrm{d}t} \sim \eta n a (\frac{\mathrm{d}R}{\mathrm{d}t})^2, \tag{9}$$

where η is the viscosity.[23] The monomer size a is hereafter set to be unity. Assuming that n monomers behave as a Gaussian statistics in the perpendicular direction to the external force, i.e. $R \sim n^{1/2}$, we obtain

$$\frac{\mathrm{d}S}{\mathrm{d}t} \sim \eta \dot{z}^2, \tag{10}$$

In a flexible polymer, we can evaluate the free energy change to be,

$$\frac{\mathrm{d}F}{\mathrm{d}t} \sim (\epsilon - \frac{l^2}{n^2})\dot{z}. \tag{11}$$

The free energy change is reversible between loading and unloading process, and therefore it does not contribute to the hysteresis. As a result, the hysteresis in a flexible polymer can be expressed as

$$A \sim \eta \dot{z} N \sim \frac{\tau_{\mathrm{R}} \dot{z}}{N}, \tag{12}$$

where τ_{R} is the Rouse relaxation time of a polymer.

In a semiflexible polymer, the collapsed parts have different structures between loading and unloading process, and therefore the free energy change contributes to the hysteresis. The free energy in a loading and unloading process can be written as the summation of three contributions; the surface, bending and volume free energy.

$$F_{\mathrm{load}} \sim \mu d_1 r_1 + l_p \frac{N-n}{r_1^2} - \epsilon(N-n), \tag{13}$$

$$F_{\mathrm{unload}} \sim \mu d_2 r_2 + l_p \frac{d_2^3}{d_2^2} - \epsilon(N-n), \tag{14}$$

where μ is the surface free energy density. A toroid is regarded as a ring with the radius r_1 and the width d_1, whereas a rod is characterized by the length r_2 and the width d_2. From the conservation of the volume of a collapsed part, the relations $d_1 \sim ((N-n)/r_1)^{1/2}$ and $d_2 \sim ((N-n)/r_2)^{1/2}$ have to be satisfied. At a given n, we may assume that the collapsed

part rapidly thermalizes, and therefore the surface and bending terms should be balanced. As a result, the free energy in a loading and unloading process is given by

$$F_{\text{load}} \sim l_p^{1/5}(N-n)^{3/5}\mu^{4/5} - \epsilon(N-n), \tag{15}$$

$$F_{\text{unload}} \sim l_p^{1/2}(N-n)^{1/2}\mu^{1/2} - \epsilon(N-n), \tag{16}$$

The entropy production in a semiflexible polymer also arises from the coiled part. Approximating that the coiled part consists of cylinders with length l_p, we estimate the entropy production as[24]

$$\frac{\mathrm{d}S}{\mathrm{d}t} \sim \frac{n}{l_p} \frac{\eta l_p}{\ln l_p}(\frac{\mathrm{d}R}{\mathrm{d}t})^2, \tag{17}$$

which is valid $l_p \gg 1$. The bending energy at the length scale n is of the order of the thermal energy $k_B T$ so that $l_p(R/n)^2 \sim 1$. As a result, we obtain

$$\frac{\mathrm{d}S}{\mathrm{d}t} \sim \frac{\eta n \dot{z}^2}{l_p \ln l_p}, \tag{18}$$

From (15), (16) and (18), the hysteresis area in a semiflexible polymer can be estimated as

$$A \sim \Delta F + \frac{\eta N^2 \dot{z}}{l_p \ln l_p}, \tag{19}$$

$$\Delta F = l_p^{1/5} N^{3/5} \mu^{4/5} - l_p^{1/2} N^{1/2} \mu^{1/2}. \tag{20}$$

When $\dot{z}$ is small, i.e., the operating speed is small (but still large such that the probability of the transition between a rod and a toroid is almost zero), the difference between the free energy change in loading and unloading process is larger than the entropy production. Therefore, the hysteresis is almost insensitive to the operating speed. The above results are qualitatively consistent with those of our simulations (Fig.3). As shown in (12), the hysteresis area in a flexible polymer decreases linearly as $\lambda = \dot{z}^{-1}$ increases. On the other hand, (19) indicates that the hysteresis in a semiflexible polymer is almost insensitive to λ when λ is large.

In this estimation, we neglect the contribution of the relaxation from a rod to a toroid as well as from a rod to a more folded rod. However, this process occurs only at small values of z and hence does not contribute to the hysteresis when N is large.

V. TWO-VARIABLE MODEL

Hysteresis is a general property of a first order phase transition.[25] However, the hysteresis described in the preceding section is different from that in the ordinary case. In a

9

semiflexible polymer, the kinetic pathway in the loading process is different from that in the unloading process. This is because different structures appear during the transition processes. Therefore, one has to consider two metastable states in the kinetics of the folding and unfolding transitions of a semiflexible polymer chain. That is, a transition from a folded state to an unfolded state occurs via one metastable state whereas the system traverses another metastable state in the reverse process. In order to represent this kind of phase transition, one has to introduce at least two variables in the kinetic equations.

In this section, we consider a model system that provides the above mentioned characteristic features. We do not intend to develop a quantitative theory specific to a semiflexible polymer chain, but rather study the hysteretic property from a general point of view based on a simple Ginzburg-Landau type approach.

We mention a recent theoretical study based on the similar idea. Bartolo et al. have investigated dynamic response of adhesion complexes by using the multidimensional energy landscape.[26] What they have found is that two alternative trajectories are possible depending on the loading rate. This is different from our concern that the system relaxes to the most stable state via two different metastable states when the process is reversed under the same loading rate.

We start with the free energy in terms of two order parameters X and Y.

$$F(X,Y) = -\frac{\mu_1}{2}X^2 - \frac{\mu_2}{2}Y^2 - \alpha XY + \frac{1}{4}X^4 + \frac{1}{4}Y^4 - h(t)X, \tag{21}$$

where μ_1, μ_2 and α are positive coefficients and h is a control parameter depending on time. For a suitable set of parameters, the free energy has four local minima, two of which correspond to folded and unfolded states. Qualitatively, the variables X and Y correspond, respectively, to the density and the orientational order of a polymer with a suitably chosen origin of the scale. The coupling between them is incorporated into the third term in the free energy (21) such that increasing the density increases the orientational order and vice versa.

The molecular dynamics simulations in the preceding section were carried out by changing the end-to-end distance at a constant speed. That is, the end-to-end distance was changed and the force exerted there was measured. To consider the corresponding situation, we regard the external parameter $h(t)$ as the end-to-end distance and assume that there is a one-to-one correspondence between the density and the force response. Under these circumstances, we

evaluate the hysteresis area in X by changing the external parameter. We fix one parameter μ_1 to be $\mu_1 = 100$ and examine two situations $\mu_1 \gg \mu_2 = 0.1$ and $\mu_1 = \mu_2 = 100$. When $\mu_2 = 0.1$, there are only two stable minima in the free energy and hence the Y variable is irrelevant and corresponds to an ordinary flexible polymer. In contrast, it will be shown below that the case with $\mu_2 = 100$ corresponds to a semiflexible polymer.

The kinetic equations for X and Y are assumed to be given, respectively, by

$$\frac{dX}{dt} = -L_1 \frac{\partial F}{\partial X} + \xi_1 = L_1(-X^3 + \mu_1 X + \alpha Y + h(t)) + \xi_1 \tag{22}$$

$$\frac{dY}{dt} = -L_2 \frac{\partial F}{\partial Y} + \xi_2 = L_2(-Y^3 + \mu_2 Y + \alpha X) + \xi_2, \tag{23}$$

where L_1 and L_2 are the Onsager coefficients. The Gaussian random forces ξ_1 and ξ_2 satisfy the fluctuation-dissipation relation,

$$< \xi_i(t)\xi_j(t') > = 2L_i k_B T \delta_{ij} \delta(t - t'). \tag{24}$$

We carried out numerical simulations for a set of Langevin equations with $L_1 = L_2 = 1$ and $\alpha = 5.0$. The external force is changed linearly in time;

$$h(t) = \pm vt + h_0, \tag{25}$$

with h_0 an initial value.

Figure 4 displays the numerical results of (22) and (23). When $\mu_2 = 0.1$, there are two stable equilibrium solutions at $(X, Y) \simeq (\pm 12, \pm 5)$. With change in the external field $h(t)$, transitions occur from one state to the other state. This corresponds to the transition between a folded state and an elongated state of a flexible polymer. In fact, the hysteresis area decreases as the inverse velocity $\dot{z}^{-1}$ is increased, as shown in Fig.5. When $\mu_2 = 100$, two metastable states appear at $(X, Y) \simeq (\pm 10, \mp 10)$ apart from the more stable states at $(X, Y) \simeq (\pm 10, \pm 10)$. The transition occurs through a different path via one of these metastable states depending on an increase or a decrease in the external field. In this case, the hysteresis area does not decrease substantially for a slow operation compared to the case with $\mu_2 = 0.1$, as shown in Fig.5. This behavior of hysteresis in Fig.5 is indeed consistent qualitatively with the results shown in Fig.3 obtained by molecular dynamics simulations.

The scale of the horizontal and vertical axes in Fig.5 is much different from that in Fig.3. This arises from the uncertainty of the relation between the density and the force response as mentioned above and from the difficulty of achieving correspondence to the time scale of the folding of a polymer in the artificial model system (22) and (23).

11

VI. SUMMARY

In summary, we have studied the force-strain relation of a bead-spring model of a polymer and found the large hysteresis in the loading-unloading cycle for a semiflexible polymer. What is different from the ordinary hysteresis is that a large hysteresis is observed even with a slow operation, which implies that there are different pathways of conformational change between folding and unfolding. This is in contrast to a flexible polymer in which the hysteresis area disappears almost entirely with a sufficiently slow operation. This means that the conformational change of a flexible polymer can be reduced essentially into a one-variable problem.

In the present paper, we have considered two limiting cases of flexible and semiflexible polymers. It would be an interesting problem to investigate systematically the change of the hysteresis by changing the bending elasticity κ. However this is left for a future study.

Although most biopolymers such as proteins have much more complicated structures, they often exhibit the characteristics of a semiflexible polymer. For example, the secondary structures such as α-helix and β-sheet parts are rather stiff and, therefore, permit a locally ordered structure. As a result, even if the initial and final states are the same, the transition paths would exhibit a large hysteresis loop, as seen in a semiflexible polymer in the present paper. Such kinetic properties are expected to play an important role in biomacromolecules.

[1] K. Svoboda and S. M. Block, Cell **77**, 773 (1994).

[2] C. Bustamante, Z. Bryant, and S. B. Smith, Nature **421**, 423 (2003).

[3] M. Takahashi, K. Yoshikawa, V. V. Vasilevskaya, and A. R. Khokhlov, J. Phys. Chem. B **101**, 9396 (1997).

[4] H. Noguchi, S. Saito, S. Kidoaki, and K. Yoshikawa, Chem. Phys. Lett. **261**, 527 (1996).

[5] M. Rief, M. Gautel, F. Oesterhelt, J. M. Frenandez, and E. Gaub, Science **276**, 1109 (1997).

[6] C. Baumann, V. Bloomfield, S. Smith, C. Bustamante, M. Wang, and S. Block, Biophys J **78**, 1965 (2000).

[7] Y. Murayama and M. Sano, J. Phys. Soc. Jpn. **70**, 345 (2001).

[8] M. Rief, J. M. Fernandez, and H. E. Gaub, Phys. Rev. Lett. **81**, 4764 (1998).

[9] H. Wada, Y. Murayama, and M. Sano, Phys. Rev. Lett. **66**, 061912 (2002).

[10] I. M. Kulić and H. Schiessel, Phys. Rev. Lett. **92**, 228101 (2004).

[11] D. Marenduzzo, A. Maritan, A. Rosa, and F. Seno, Eur. Phys. J. E **15**, 83 (2004).

[12] C. Jarzynski, Phys. Rev. Lett. **78**, 2690 (1997).

[13] G. E. Crooks, J. Stat. Phys **90**, 1481 (1998).

[14] G. Hummer and A. Szabo, Proc. Natl. Acad. Sci. USA **98**, 3658 (2001).

[15] T. Sakaue and K. Yoshikawa, J. Chem. Phys. **117**, 6323 (2002).

[16] R. G. Winkler, J. Chem. Phys. **118**, 2919 (2003).

[17] B. Y. Ha and D. Thirumalai, J. Chem. Phys. **102**, 9408 (1995).

[18] N. Saito, K. Takahashi, and Y. Yasuo, J. Phys. Soc. Jpn. **22**, 219 (1967).

[19] K. Yoshikawa and Y. Matsuzawa, J. Am. Chem. Soc. **118**, 929 (1996).

[20] P.-C. Li and D. E. Makarov, J. Chem. Phys. **119**, 9260 (2003).

[21] A. Halperin and B. Zhulina, Europhys. Lett. **15**, 417 (1991).

[22] M. Wittkop and D. Göritz, Phys. Rev. E **53**, 838 (1996).

[23] A. Halperin and P. M. Goldbart, Phys. Rev. E **61**, 565 (2000).

[24] M. Doi and S. Edwards, *The Theory of Polymer Dynamics* (Clarendon, Oxford, 1986).

[25] L. D. Landau and E. M. Lifshitz, *Statistical Physics* (Pergamon, London, 1958).

[26] D. Bartolo, I. Derényi, and A. Adjdari, Phys. Rev. E **65**, 051910 (2002).
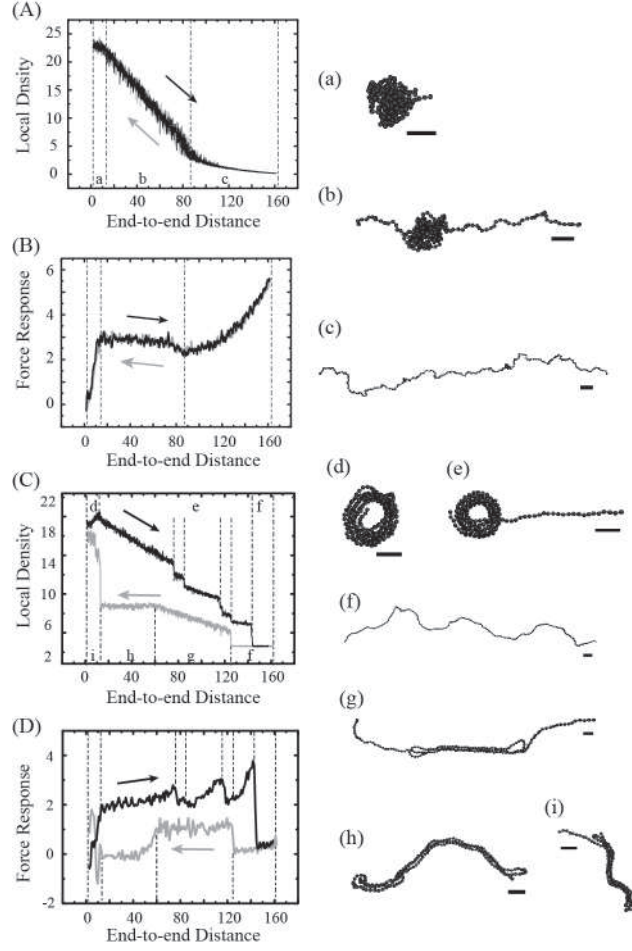
Figures

FIG. 1: Local monomer density and force response under strain in flexible (A, B) and semiflexible (C, D) polymers. The black and gray lines show loading and unloading processes respectively. Typical snapshots of chain conformation are also shown. The scale bar corresponds to $5a$.
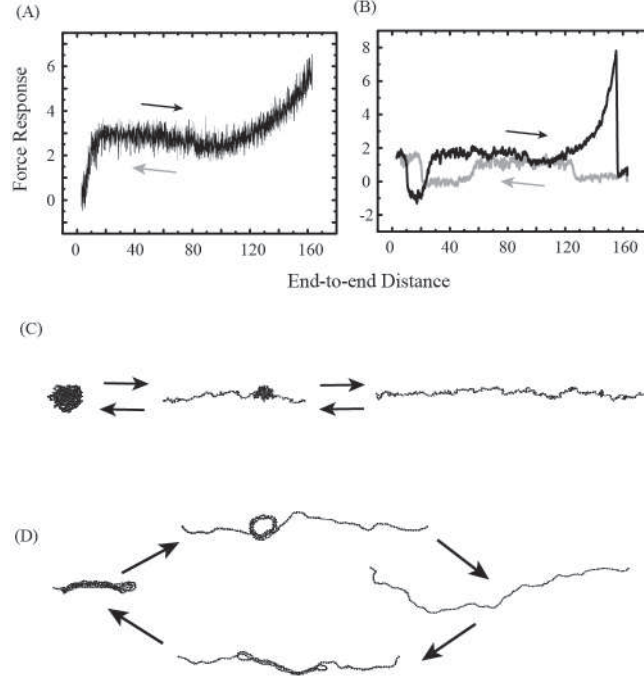
15

FIG. 2: Force response in flexible (A) and semiflexible (B) polymers. While the transition pathways in loading and unloading processes are the same for a flexible polymer (C), for a semiflexible polymer the pathway in loading is largely different from that in unloading (D).
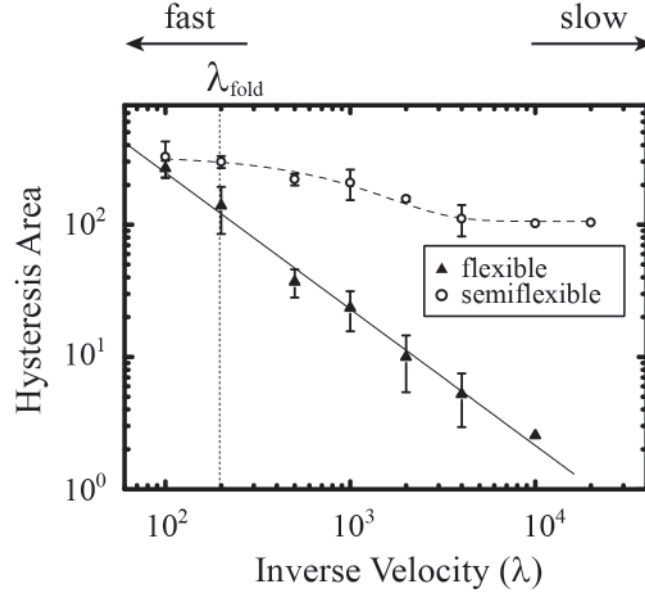
FIG. 3: Inverse velocity dependence on hysteresis in flexible (closed triangles) and semiflexible (open circles) polymers in our simulations. The solid and broken lines are guides to eyes.
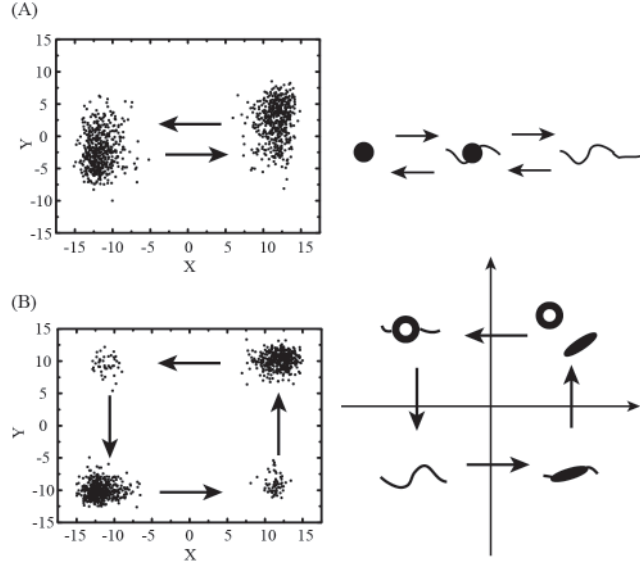
FIG. 4: Time trajectory of our model calculation in the XY plane for $\mu_2 = 0.1$ (A) and $\mu_2 = 100$ (B), and schematic representations of the correspondence to our simulation results in Fig. 2 (C) and (D).
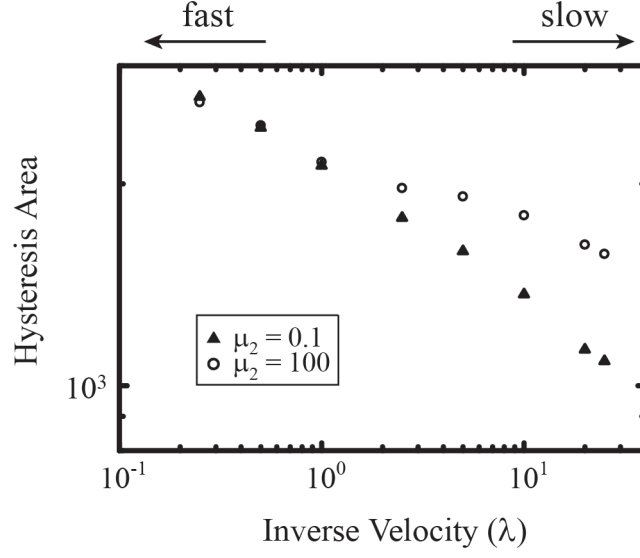
FIG. 5: Inverse velocity dependence on hysteresis at $\mu_2 = 0.1$ (closed triangles) and $\mu_2 = 100$ (open circles) obtained from (22) and (23).